IEEE Access
Multidisciplinary | Rapid Review | Open Access Journal

Received July 25, 2019, accepted August 5, 2019, date of publication August 14, 2019, date of current version September 18, 2019.

Digital Object Identifier 10.1109/ACCESS.2019.2935237

Nonlinear Control of Active Four Wheel Steer-By-Wire Vehicles

SHUYOU YU[1,2], (Member, IEEE), WENBO LI[2], WUYANG WANG[2], AND TING QU[1,2]
[1]State Key Laboratory of Automotive Simulation and Control, Jilin University, Changchun 130022, China
[2]College of Communication Engineering, Jilin University, Changchun 130022, China

Corresponding author: Ting Qu (quting@jlu.edu.cn)

This work was supported in part by the National Natural Science Foundation of China under Grant 61573165 and Grant 61703178, in part by the Sino-Korean Cooperation Project of the National Natural Science Foundation of China under Grant 6171101085, in part by the Jilin Provincial Science Foundation of China under Grant 20180520200JH, in part by the Joint Project of Jilin University under Grant SXGJSF2017-2-1-1, and in part by the Department of Education, Jilin Province, China (Project of active four-wheel steer-by-wire vehicles).

ABSTRACT In this paper, a nonlinear triple-step steering controller for four wheel steer-by-wire vehicles has been presented to enhance handling stability. The proposed nonlinear triple-step steering controller commands the front and rear steering angles so as to track both the reference yaw rate and sideslip angle. Thus, it can effectively improve the tracking accuracy even if tyres of vehicles are working in extremely nonlinear region. Considering the influence of the driver on the handling stability, a PID driver model is introduced. Both open-loop and closed-loop simulations are carried out in CarSim.

INDEX TERMS Four wheel steer-by-wire vehicle, handling stability, triple-step method, map.

I. INTRODUCTION

Improving vehicle stability is a promising solution to road safety which is an important issue of the automobile industry. Therefore, the chassis control technology which can improve the stability of vehicles has been widely concerned. According to the longitudinal, vertical and lateral dynamics of the vehicle, the chassis control technology can be divided into three categories. Anti-lock braking system is one of the most effective active safety control systems for vehicles, since it can keep the rotational wheel from locking, and consequently guarantee the braking safety and handling stability [1], [2]. The anti-slip regulation can improve the adhesion of the vehicle to the ground during rapid change of speed, preventing the wheel from slipping and avoiding the risk of lateral sliding [3], [4]. Aiming at the braking energy feedback control of the electric vehicle, a regenerative braking torque distribution strategy is developed under different speeds and braking conditions [5]. A main-servo loop control structure is proposed [6], the main loop calculates and allocates the aim force by the optimal robust control algorithm and the servo loop tracks the target force by the onboard independent brake actuators. Considering the problem of ride height tracking for an active air suspension system which has parametric uncertainties, a robust ride height controller is proposed [7], the ride height can converge on a neighborhood of the desired height, achieving global uniform ultimate boundedness. According to the single degree-of-freedom nonlinear suspension system under primary resonance conditions, a pair of symmetric linear viscoelastic end-stops is proposed [8].

In addition, the steering technology can also improve vehicle stability. According to the problem of different road friction coefficients, a neurofuzzy controller is proposed in [9]. Then the trained fuzzy controller is applied to a vehicle with active front steering system to improve vehicle handling stability. A nonlinear adaptive observer is proposed to ensure the stability by estimating the friction coefficient [10]. Due to its flexible steering mode, four wheel steering (4WS) technology has attracted extensive attention since it can effectively improve vehicle handling stability and active safety [11]. Active rear wheel steering technology is a mature four wheel steering technology which has been successfully applied in real vehicles [12], [13]. However, the active rear wheel steering system is a typical single-input single-output system: only one input variable of rear wheel angle and one state variable of sideslip angle or yaw rate. The system actuators are of high price and high quality and can easily be replaced by lateral yaw controller and electronic stability controller [14]–[16]. In recent years, with the development of vehicle electronic, intelligence and integration, steer-by-wire has been widely used in the automobile field [17]–[19]. The active four wheel

The associate editor coordinating the review of this article and approving it for publication was Zheng H. Zhu.

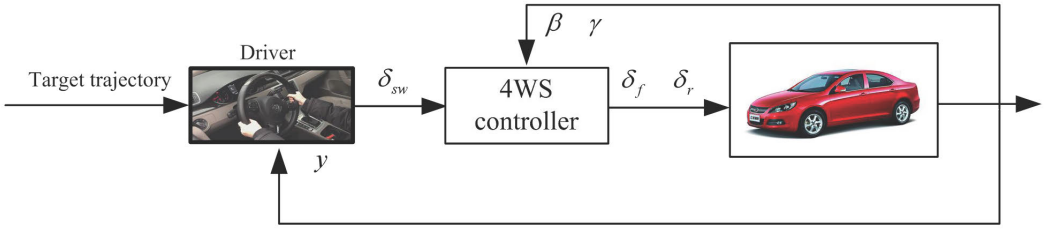

FIGURE 1. 4WS vehicle control system.

steer-by-wire system breaks through the limitation that the lateral acceleration gain and yaw velocity steady state gain change greatly when the vehicle speed and the front wheel angle change, and effectively improves the vehicle steering characteristics by control of the front and rear wheel angle simultaneously [20]. Considering the delay of the saturated actuator, an internal mode decoupling scheme is adopted to improve the anti-interference ability of the system [21]. A sliding mode control of active four wheel steering systems is proposed in [22], where an integral time-variant sliding surface is adopted to eliminate steady state errors, and a smooth function is used to alleviate the chattering effect. Considering the inner coupling between the active front and rear wheels of four-wheel steering vehicles, a double-layer dynamic decoupling control system composed of the dynamic decoupling unit and the steering control unit is proposed in [23]. In order to reduce the influence of uncertainty such as lateral wind disturbance and vehicle quality change, a linear triple-step controller is designed to implement the accurate tracking of the ideal reference [24]. A disturbance observer is presented in [25], where the front and rear wheel steering angles are controlled simultaneously to follow both the desired sideslip angle and yaw rate by combination of feedforward control and feedback control. A disturbance observer based quasi full information feedback control law of linear systems is proposed in [26]. The feedback control law is with direct measurement of the plant states and the estimation of the disturbances. A mixed H_2/H_∞ robust control method is proposed with the optimized weighting functions to guarantee system performance, robustness, and the robust stability [27].

When the lateral acceleration of the vehicle is large in extreme handling situations, the tyre lateral characteristic will enter the nonlinear region. Neural network is used to design a 4WS control system by actively controlling the rear wheel rotation angle [28]. An adaptive controller was designed based on the two degree-of-freedom vehicle model, where the tyre stiffness was adaptively estimated to compensate the nonlinearity of tyre lateral force [29]. Based on the Takagi-Sugeno fuzzy model which is established to represent the nonlinear characteristic, a robust adaptive sliding mode controller is designed to achieve the path tracking and vehicle lateral control simultaneously [30]. It is emphasized that most control methods are only used for the evaluation of vehicle state responses. As the driver will modify his driving characteristics according to the vehicle's states, it is insufficient to evaluate its handling stability only from vehicle's responses [31].

The main contributions of this paper are as follows: 1) The nonlinear triple-step control strategy is applied to the active four wheel steer-by-wire vehicle. The control structure of feedforward-feedback is adopted. 2) A "human-vehicle-road" closed-loop system is established, which takes the factor of drivers into consideration.

The paper is organized as follows. Section II derives the dynamic model of the active four-wheel steering system and set-up the control problems. Section III introduces the design process of the nonlinear triple-step controller of the active four wheel steer-by-wire system. Section IV verifies the effectiveness of the proposed controller through open-loop and closed-loop simulation. Some conclusions are shown in Section V.

II. PROBLEM SETUP

The purpose is to track the ideal steering characteristics, and to improve the vehicle handling stability. As shown in Fig.1, the driver applies a steering wheel angle to track the target trajectory, and converts the steering wheel angle into a reference front wheel angle input.

Suppose that the yaw rate of the active four wheel steer-by-wire vehicle is measurable, and the centroid side angle can be accurately estimated.

A. VEHICLE MODEL

The lateral acceleration, yaw rate and centroid sideslip angle of vehicles have strong connection with mass, speed, yaw moment of inertia and tyre cornering stiffness. The ideal vehicle model has two degree-of-freedom, i.e., yaw and sideslip motions, shown in Fig.2.

In order to establish the two degree-of-freedom model, the following assumptions are made [32]: (1) The impact of the suspension and steering mechanisms is negligible. The vehicle has only a uniform longitudinal movement parallel to the ground. (2) The wheel is only affected by the tyre lateral force, i.e., the left and right tyres have the same lateral characteristics. (3) The vehicle travels on the road surface with a uniform adhesion coefficient.

According to Newton's Second Law, the two degree-of-freedom kinematics equation of the active four-wheel

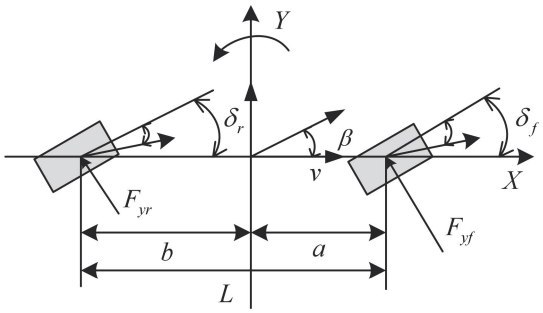

FIGURE 2. Two degree-of-freedom vehicle model.

steering vehicle is [11]:

$$\begin{aligned} mv\left(\dot{\beta}+\gamma\right) &= F_{yf}+F_{yr} \\ I_z\dot{\gamma} &= aF_{yf}-bF_{yr} \end{aligned} \tag{1}$$

where β is the sideslip angle in the vehicle body, m is the vehicle mass, v is the longitudinal speed, a is the distance from the center of gravity to the front axle, b is the distance from the center of gravity to the rear axle, γ is the yaw rate in the vehicle body, I_z is the yaw moment of inertia, and F_{yf} and F_{yr} are tyre lateral forces respectively.

B. TYRE MODEL

Vehicle dynamics is closely related to tire characteristics while the effects of air resistance and gravity are neglected [32]. In extreme handling situations, a rational model with validity extending beyond the linear regime of the tyre should be considered. Tyre lateral force can be expressed as

$$F_y\left(\alpha,\lambda,\mu,F_z\right) \approx \frac{\mu F_z}{\mu_0 F_{z0}} \frac{\gamma_z}{\gamma_\lambda \lambda^2+1} \frac{C_\alpha}{\gamma_\alpha \alpha^2+1}\alpha \tag{2}$$

where F_z is the vertical load, F_{z0} is the nominal tyre load, μ is the road adhesion coefficient, μ_0 is the nominal road adhesion coefficient, λ is the longitudinal slip, C_α is the tyre cornering stiffness, α is the tyre slip angle and γ_z, γ_λ, γ_α are data of the tyre obtained from the experiment.

Since this paper only studies the yaw and sideslip movement of the vehicle, i.e., ignoring the longitudinal influence, the following simplifications are made:

1) Longitudinal slip terms are chosen as zero.
2) Road adhesion coefficient is taken as μ_0, i.e., only dry road is considered.
3) Shape factors γ_z and γ_λ can be merged into a single factor $\gamma_\alpha = \left(\frac{1}{\alpha^*}\right)$ where α^* is tyre slip angle.

The tyre slip angles are

$$\begin{aligned} \alpha_f &= \beta+\frac{a\gamma}{v}-\delta_f \\ \alpha_r &= \beta-\frac{b\gamma}{v}-\delta_r \end{aligned} \tag{3}$$

where δ_f, δ_r are inputs for the front and rear wheel angles, respectively.

Choose the state variable as $x = \left[\beta\ \gamma\right]^T$ and the control input $u = \left[\delta_f\ \delta_r\right]^T$, the two degree-of-freedom active four wheel steer-by-wire vehicle are derived

$$\begin{aligned} \dot{\beta} &= \frac{F_{yf}\left(\beta,\gamma,\delta_f\right)+F_{yr}\left(\beta,\gamma,\delta_r\right)}{mv}-\gamma \\ \dot{\gamma} &= \frac{aF_{yf}\left(\beta,\gamma,\delta_f\right)-bF_{yr}\left(\beta,\gamma,\delta_r\right)}{I_z} \end{aligned} \tag{4}$$

III. STRUCTURE OF THE NONLINEAR STEERING CONTROLLER

The control objective is to ensure that the vehicle's actual centroid sideslip angle and yaw rate can track the desired centroid sideslip angle and yaw rate, i.e., $\beta=\beta^*$, $\gamma=\gamma^*$. As shown in Fig.3, the reference model gives the ideal centroid sideslip angle and yaw rate. Steady-state-like control ($f_s\left(\beta,\gamma\right)$) ensures that the system can reach its steady state. Feedforward control considering the variation of the reference signal $\left(f_f\left(\beta,\gamma,\dot{\beta}^*,\dot{\gamma}^*\right)\right)$ is used to compensate the influence of reference dynamic on the system. State-dependent error feedback control ($f_e\left(\beta,\gamma,\Delta\beta,\Delta\gamma\right)$) is used to minimize the tracking error, eliminate the influence of uncertainty and improve the robustness of the system [33].

A. REFERENCE MODEL

The ideal steering characteristics of the active four wheel steering vehicle ensures that the system has the steering sensitivity consistent with the traditional front wheel steering vehicle. In other words, the steady state gain of yaw rate is required to be the same as that of traditional front wheel steering vehicles, and the centroid sideslip angle is close to zero [34].

Ideal yaw rate γ^* adopts a first-order system to reduce the influence of input mutation on steering sensitivity

$$\gamma^* = \frac{k_r}{1+\tau_r s}\delta_{sw} \tag{5}$$

where

$$k_r = \frac{C_f C_r\left(a+b\right)v}{C_f C_r(a+b)^2+mv^2\left(aC_f-bC_r\right)} \tag{6}$$

is the steady state gain of the ideal yaw rate, C_f and C_r are the front and rear wheel side cornering stiffness, τ_r is the time constant and δ_{sw} is the ideal front wheel angle.

The ideal sideslip angle β^* is

$$\beta^* = \frac{k_\beta}{1+\tau_\beta s}\delta_{sw} \tag{7}$$

where k_β is the ideal centroid sideslip angle gain and τ_β is the time constant of the ideal yaw rate.

Define $x_d = \left[\beta^*\ \gamma^*\right]^T$ as the state variable of the reference model and $u_d = \delta_{sw}$ as the input of the reference model. Then, dynamics of the ideal reference model is

$$\dot{x}_d = A_d x_d + B_d u_d \tag{8}$$

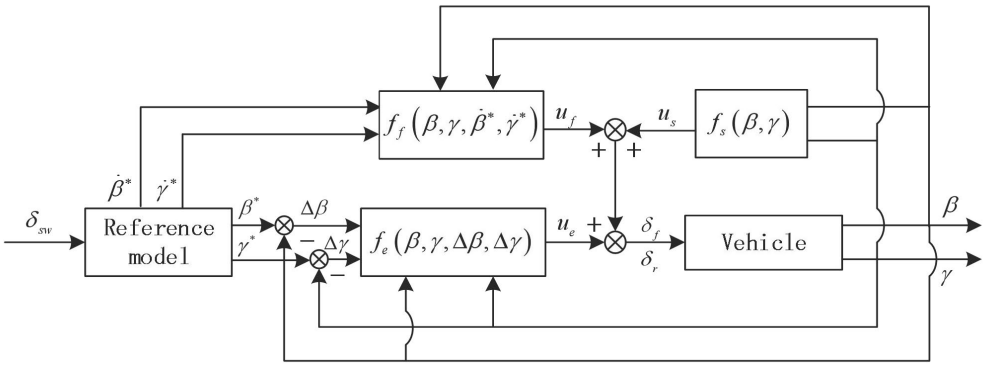

FIGURE 3. The structure of controller.

with

$$A_d = \begin{bmatrix} -\frac{1}{\tau_\beta} & 0 \\ 0 & -\frac{1}{\tau_\beta} \end{bmatrix}, \quad B_d = \begin{bmatrix} \frac{k_\beta}{\tau_\beta} \\ \frac{k_\gamma}{\tau_\gamma} \end{bmatrix} \tag{9}$$

B. THE NONLINEAR TRIPLE-STEP CONTROLLER

1) STEADY-STATE-LIKE CONTROL

In the field of automotive engineering, maps are often used to characterize input-output relationships at steady state. Accordingly, a control input is obtained by checking reversely a map [35]–[37].

Denote $u_s = [u_{1s}\ \ u_{2s}]^T$ as the control input while sideslip angular velocity $\dot{\beta} = 0$ and yaw acceleration $\dot{\gamma} = 0$, then

$$F_{yf}(\beta, \gamma, u_{1s}) + F_{yr}(\beta, \gamma, u_{2s}) = mv\gamma \tag{10}$$

$$aF_{yf}(\beta, \gamma, u_{1s}) = bF_{yr}(\beta, \gamma, u_{2s}) \tag{11}$$

That is,

$$F_{yf}(\beta, \gamma, u_{1s}) = \frac{bmv\gamma}{a+b} \tag{12}$$

$$F_{yr}(\beta, \gamma, u_{2s}) = \frac{amv\gamma}{a+b} \tag{13}$$

Therefore, the steady-state-like control is obtained by looking up Fig.4 and Fig.5

$$\begin{aligned} u_{1s} &= {F_{yfmap}}^{-1}\left(\frac{bmv\gamma}{a+b}\right) \\ u_{2s} &= {F_{yrmap}}^{-1}\left(\frac{amv\gamma}{a+b}\right) \end{aligned} \tag{14}$$

where ${F_{yfmap}}^{-1}$ and ${F_{yrmap}}^{-1}$ represent the front tyre lateral force and the rear tyre lateral force at steady state, respectively. The steady-state-like control regulates a dynamic system to its operating point (steady state), which plays a major role in regulation task. Note that the tyre lateral force at steady state is a continuous function of the slip angle, cf. Fig.4 and Fig.5.

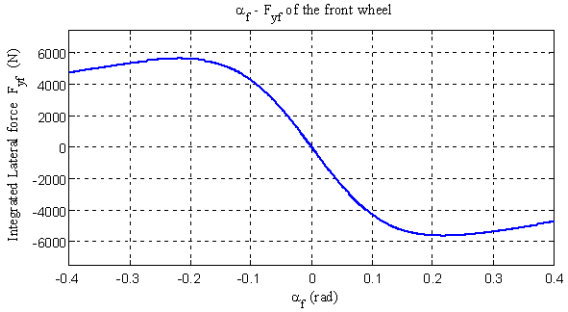

FIGURE 4. Front Tyre Lateral Force - Slip Angle Curve.

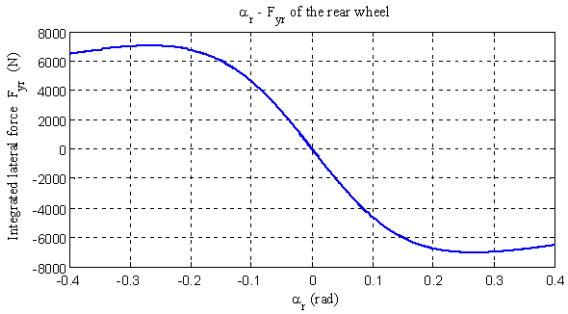

FIGURE 5. Rear Tyre Lateral Force - Slip Angle Curve.

2) FEEDFORWARD CONTROL

Denote the feedforward control of the reference dynamic is $u_f = [u_{1f}\ \ u_{2f}]$ [38].

According to the tracking condition of the reference dynamic $\dot{\beta} = \dot{\beta}^*, \dot{\gamma} = \dot{\gamma}^*$, the following results can be obtained.

$$\begin{aligned} \dot{\beta} &= \frac{F_{yf}(\beta, \gamma, u_{1s}+u_{1f}) + F_{yr}(\beta, \gamma, u_{2s}+u_{2f})}{mv} - \gamma \\ &= \dot{\beta}^* = 0 \\ \dot{\gamma} &= \frac{aF_{yf}(\beta, \gamma, u_{1s}+u_{1f}) - bF_{yr}(\beta, \gamma, u_{2s}+u_{2f})}{I_z} \\ &= \dot{\gamma}^* \end{aligned} \tag{15}$$

By Taylor expansion at the point of u_{1s} and u_{2s}, F_{yf} and F_{yr} can be rewritten as

$$\begin{aligned} F_{yf}\left(\beta,\gamma,u_{1s}+u_{1f}\right) &= F_{yf}\left(\beta,\gamma,u_{1s}\right)+\left.\frac{\partial F_{yf}}{\partial u_1}\right|_{u_{1s}} u_{1f} \\ F_{yr}\left(\beta,\gamma,u_{2s}+u_{2f}\right) &= F_{yr}\left(\beta,\gamma,u_{2s}\right)+\left.\frac{\partial F_{yr}}{\partial u_2}\right|_{u_{2s}} u_{2f} \end{aligned} \tag{16}$$

Substituting Eq.(16) into Eq.(15), it can be obtained that

$$\begin{aligned} &\frac{1}{mv}\left(\left.\frac{\partial F_{yf}}{\partial u_1}\right|_{u_{1s}} u_{1f}+\left.\frac{\partial F_{yr}}{\partial u_2}\right|_{u_{2s}} u_{2f}\right)=0 \\ &\dot{\gamma}^*=\frac{1}{I_z}\left(a\left.\frac{\partial F_{yf}}{\partial u_1}\right|_{u_{1s}} u_{1f}-b\left.\frac{\partial F_{yr}}{\partial u_2}\right|_{u_{2s}} u_{2f}\right) \end{aligned} \tag{17}$$

Therefore, a simplified feedforward control of the reference dynamic u_f can be obtained

$$\begin{aligned} u_{1f} &= \frac{\dot{\gamma}^* I_z}{(a+b)\left.\frac{\partial F_{yf}}{\partial u_1}\right|_{u_{1s}}} \\ u_{2f} &= \frac{-\dot{\gamma}^* I_z}{(a+b)\left.\frac{\partial F_{yr}}{\partial u_2}\right|_{u_{2s}}} \end{aligned} \tag{18}$$

3) STATE-DEPENDENT ERROR FEEDBACK CONTROL

Denote the error feedback control law as $u_e = [u_{1e}\ \ u_{2e}]^T$. The control law of the triple-step controller is

$$u = u_s(x) + u_f(x) + u_e(x) \tag{19}$$

Then the following results can be obtained

$$\begin{aligned} &\dot{\beta} \\ &= \frac{F_{yf}\left(\beta,\gamma,u_{1s}+u_{1f}+u_{1e}\right)+F_{yr}\left(\beta,\gamma,u_{2s}+u_{2f}+u_{2e}\right)}{mv}-\gamma \\ &\dot{\gamma} \\ &= \frac{aF_{yf}\left(\beta,\gamma,u_{1s}+u_{1f}+u_{1e}\right)-bF_{yr}\left(\beta,\gamma,u_{2s}+u_{2f}+u_{2e}\right)}{I_z} \end{aligned} \tag{20}$$

By Taylor expansion at the point of u_{1s} and u_{2s} again, F_{yf} and F_{yr} can be rewritten as

$$\begin{aligned} &F_{yf}\left(\beta,\gamma,u_{1s}+u_{1f}+u_{1e}\right) \\ &\quad = F_{yf}\left(\beta,\gamma,u_{1s}\right)+\left.\frac{\partial F_{yf}}{\partial u_1}\right|_{u_{1s}}\left(u_{1f}+u_{1e}\right) \\ &F_{yr}\left(\beta,\gamma,u_{2s}+u_{2f}+u_{2e}\right) \\ &\quad = F_{yr}\left(\beta,\gamma,u_{2s}\right)+\left.\frac{\partial F_{yr}}{\partial u_2}\right|_{u_{2s}}\left(u_{2f}+u_{2e}\right) \end{aligned} \tag{21}$$

Substitute Eq.(21) into Eq.(20)

$$\begin{aligned} \dot{\beta} = &\frac{F_{yf}\left(\beta,\gamma,u_{1s}\right)+\left.\frac{\partial F_{yf}}{\partial u_1}\right|_{u_{1s}}\left(u_{1f}+u_{1e}\right)}{mv} \\ &+\frac{F_{yr}\left(\beta,\gamma,u_{2s}\right)+\left.\frac{\partial F_{yr}}{\partial u_2}\right|_{u_{2s}}\left(u_{2f}+u_{2e}\right)}{mv}-\gamma \end{aligned}$$

$$\begin{aligned} \dot{\gamma} = &\frac{a\left(F_{yf}\left(\beta,\gamma,u_{1s}\right)+\left.\frac{\partial F_{yf}}{\partial u_1}\right|_{u_{1s}}\left(u_{1f}+u_{1e}\right)\right)}{I_z} \\ &-\frac{b\left(F_{yr}\left(\beta,\gamma,u_{2s}\right)+\left.\frac{\partial F_{yr}}{\partial u_2}\right|_{u_{2s}}\left(u_{2f}+u_{2e}\right)\right)}{I_z} \end{aligned} \tag{22}$$

Define the tracking error as

$$\begin{aligned} e &= x_d - x \\ &= \left[\beta^*-\beta \quad \gamma^*-\gamma\right]^T \end{aligned} \tag{23}$$

Denote the error of the centroid sideslip angle and the error of the yaw rate error as $e_\beta = \left[\beta^*-\beta\right], e_\gamma = \left[\gamma^*-\gamma\right]$, respectively.

Then,

$$\begin{aligned} \dot{e}_\beta &= \dot{\beta}^*-\dot{\beta} \\ &= -\frac{1}{mv}\left(\left.\frac{\partial F_{yf}}{\partial u_1}\right|_{u_{1s}} u_{1e}+\left.\frac{\partial F_{yr}}{\partial u_2}\right|_{u_{2s}} u_{2e}\right) \\ \dot{e}_\gamma &= \dot{\gamma}^*-\dot{\gamma} \\ &= -\frac{1}{I_z}\left(a\left.\frac{\partial F_{yf}}{\partial u_1}\right|_{u_{1s}} u_{1e}-b\left.\frac{\partial F_{yr}}{\partial u_2}\right|_{u_{2s}} u_{2e}\right) \end{aligned} \tag{24}$$

Rewrite Eq.(24) as

$$\begin{bmatrix}\dot{e}_\beta \\ \dot{e}_\gamma\end{bmatrix}=\begin{bmatrix}-b_{11} & -b_{12} \\ -b_{21} & -b_{22}\end{bmatrix}\begin{bmatrix}u_{1e} \\ u_{2e}\end{bmatrix} \tag{25}$$

where

$$\begin{aligned} b_{11} &= \frac{1}{mv}\left.\frac{\partial F_{yf}}{\partial u_1}\right|_{u_{1s}} \quad b_{12} = \frac{1}{mv}\left.\frac{\partial F_{yr}}{\partial u_2}\right|_{u_{2s}} \\ b_{21} &= \frac{1}{I_z}a\left.\frac{\partial F_{yf}}{\partial u_1}\right|_{u_{1s}} \quad b_{22} = -\frac{1}{I_z}b\left.\frac{\partial F_{yr}}{\partial u_2}\right|_{u_{2s}} \end{aligned} \tag{26}$$

Suppose the designed error feedback control law is

$$\begin{bmatrix}u_{1e} \\ u_{2e}\end{bmatrix}=K\begin{bmatrix}e_\beta \\ e_\gamma\end{bmatrix} \tag{27}$$

where $K=\begin{bmatrix}k_{11} & k_{12} \\ k_{21} & k_{22}\end{bmatrix}$ is a control gain.

Substituting Eq.(27) into Eq.(25), then the dynamics of the tracking error is

$$\begin{bmatrix}\dot{e}_\beta \\ \dot{e}_\gamma\end{bmatrix}=\begin{bmatrix}-b_{11} & -b_{12} \\ -b_{21} & -b_{22}\end{bmatrix}K\begin{bmatrix}e_\beta \\ e_\gamma\end{bmatrix} \tag{28}$$

Define

$$z=\begin{bmatrix}-b_{11} & -b_{12} \\ -b_{21} & -b_{22}\end{bmatrix}\begin{bmatrix}k_{11} & k_{12} \\ k_{21} & k_{22}\end{bmatrix} \tag{29}$$

If the characteristic root of z have a negative real part, then the second-order system (28) is asymptotically stable. Determine

$$\begin{aligned} k_{11} &= \frac{b_{22}}{b_{12}b_{21}-b_{11}b_{22}}k_1 \quad k_{12} = \frac{-b_{12}}{b_{11}b_{22}-b_{12}b_{21}}k_2 \\ k_{21} &= \frac{b_{21}}{b_{12}b_{21}-b_{11}b_{22}}k_1 \quad k_{22} = \frac{-b_{11}}{b_{11}b_{22}-b_{12}b_{21}}k_2 \end{aligned}$$

TABLE 1. Vehicle parameters.

parameter	value
Vehicle quality m/kg	1704.7
Distance from centroid to front axle a/m	1.035
Distance from centroid to rear axle b/m	1.665
Yaw moment of inertia $I_z/(kg \cdot m^2)$	3048.1
Front wheel cornering stiffness $C_f/(N \cdot rad^{-1})$	39515.0
Rear wheel cornering stiffness $C_r/(N \cdot rad^{-1})$	39515.0

with $k_1 > 0$ and $k_2 > 0$, then

$$\begin{aligned} \dot{e}_\beta &= -k_1 e_\beta \\ \dot{e}_\gamma &= -k_2 e_\gamma \end{aligned} \tag{30}$$

The overall control law of the triple-step controller is:

$$u = u_s + u_f + u_e. \tag{31}$$

Considering the parameter-varying property of tire cornering stiffness in extreme handling situations, the design process achieves decoupling of multi-input and multi-output systems and reduces the workload of controller parameter calibration. From the form of the control law, each part of the control law contains the system output state and change parameters, and realizes the self-regulation of the control law parameters.

IV. SIMULATIONS

CarSim is a professional software developed by American Mechanical Simulation Company for analyzing vehicle system dynamics with high simulation accuracy. The simulation scenario of the vehicle in CarSim is described as follows: The vehicle travels on the flat ground without obstacles, and only performs turning operation to test the stability of the vehicle.

In order to verify the effectiveness of the proposed scheme, both front wheel steering vehicle and the proportional controller are designed to compare with. The ratio of the proportional controller is [24], [39]

$$\frac{\delta_f}{\delta_r} = \frac{-b + mav^2/C_f\,(a+b)}{a + mbv^2/C_r\,(a+b)}$$

The parameters of the error feedback control are $k_1 = 500$ and $k_2 = 800$. The vehicle is a D-class sedan in CarSim and the vehicle parameters are shown in Table.1.

A. OPEN-LOOP TEST

Here, both the step response and the continuous sinusoidal test are carried out in CarSim.

1) CORNERING MANEUVER

Scenario: the vehicle is traveling in a straight line at a constant speed $20m/s$, the steering wheel turns a fixed angle. As shown in Fig.6, the amplitude of the front wheel rotation angle is 5° ($0.0872rad$).

Responses of vehicles are shown in Fig.7-Fig.10, in which Fig.7 and Fig.8 are the changes of the vehicle's centroid sideslip angle and yaw rate. Both the centroid sideslip angle

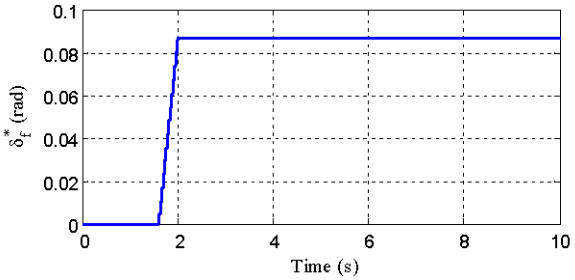

FIGURE 6. Reference front wheel steering angle input.

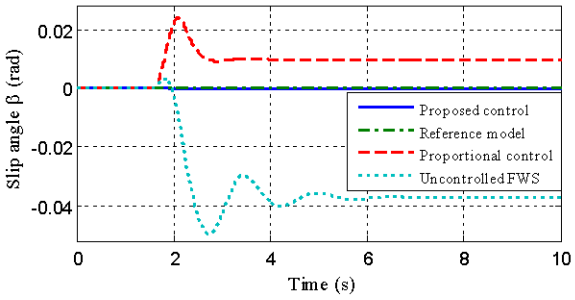

FIGURE 7. Slip angle responses.

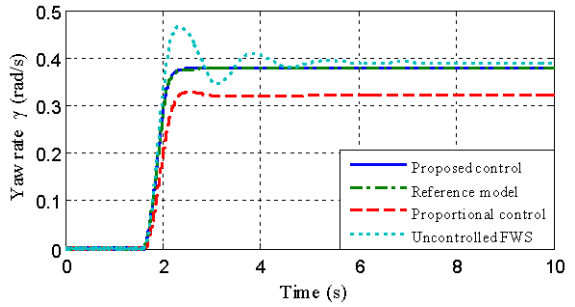

FIGURE 8. Yaw rate responses.

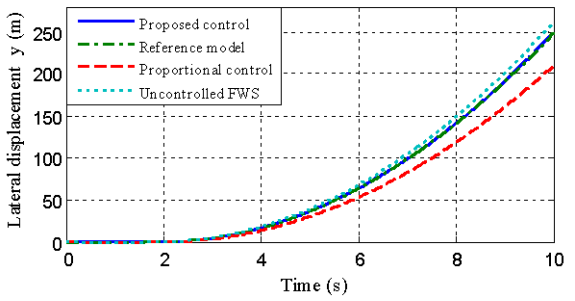

FIGURE 9. Lateral displacement responses.

and the yaw rate of four wheel steering vehicles with proportional controller are close to the references. However, the yaw rate is less than the related ideal reference, which will result in the so called excessive steering problem. The dynamics of the centroid sideslip angle of the front wheel steering vehicle is of stability, oscillation and overshoot. In general, oscillation and overshoot have negative influence on the handling stability. It can be seen from Fig.11 that the front and rear wheel

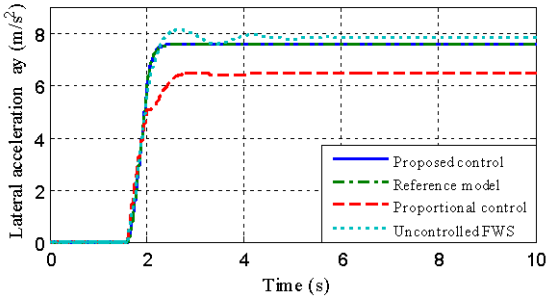

FIGURE 10. Lateral acceleration responses.

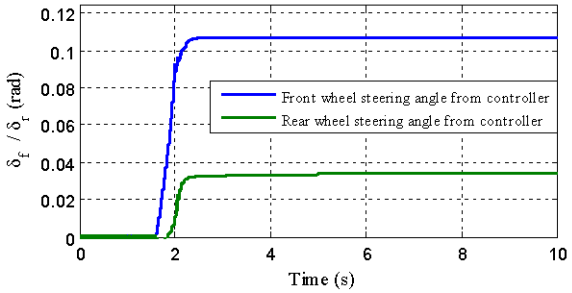

FIGURE 11. Front/Rear steering angle from controller.

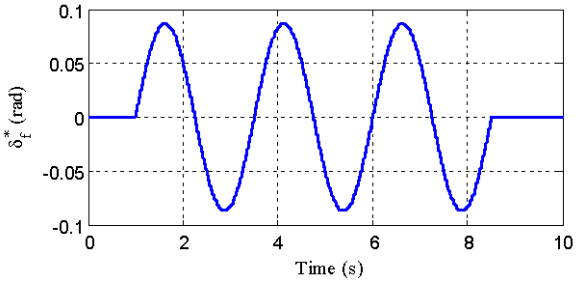

FIGURE 12. Reference front wheel steering angle input.

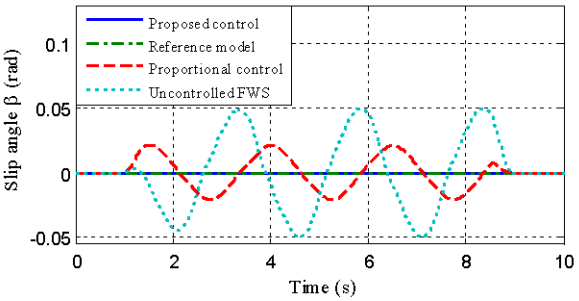

FIGURE 13. Slip angle responses.

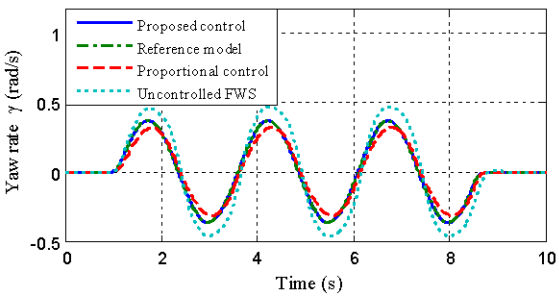

FIGURE 14. Yaw rate responses.

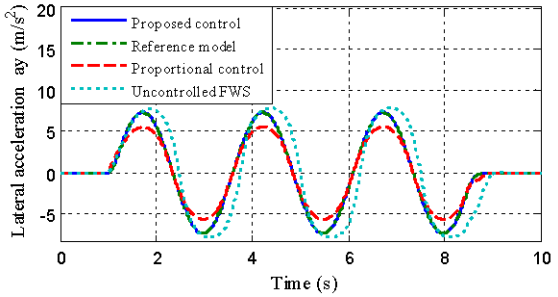

FIGURE 15. Lateral acceleration responses.

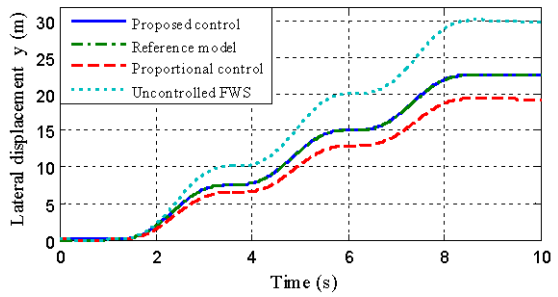

FIGURE 16. Lateral displacement responses.

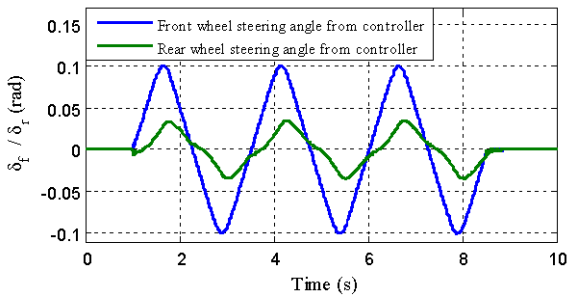

FIGURE 17. Front/Rear steering angle from controller.

rotation angles given by the triple-step controller are all within a reasonable range.

2) SINUSOIDAL STEERING ANGLE

Scenario: Sinusoidal maneuver with the amplitude 5° and the frequency $2.512 rad/s$ is carried out while the vehicle is travelling at a velocity of $20 m/s$, c.f., Fig.12.

Responds of vehicles are shown in Fig.13-Fig.16. Compared with the other schemes, the triple-step controller achieves the best tracking effect on the the ideal steering characteristic. The yaw rate of the vehicle under proportional control is less than that of the front wheel steering vehicle. Thus, it may change the driving feeling. It can be seen from Fig.17 that the front and rear wheel angle is reasonable and there is no actuator saturation.

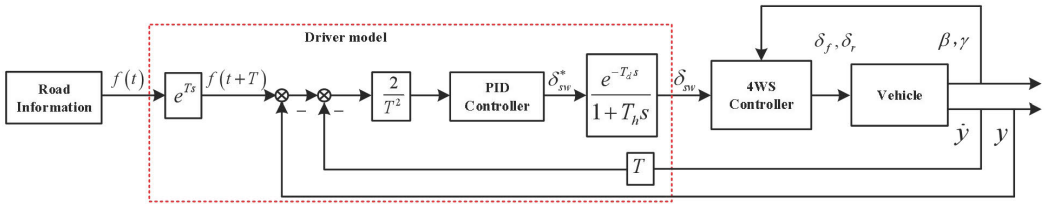

FIGURE 18. The closed-loop system based on preview optimal curvature driver model.

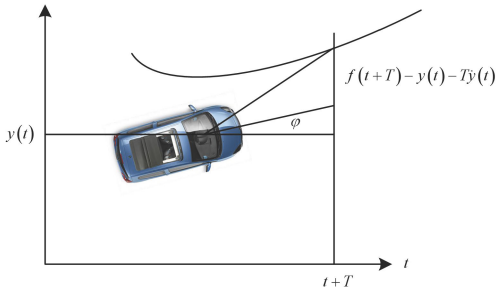

FIGURE 19. Deviation diagram of driving trajectory.

B. CLOSED-LOOP TEST

In this section, the driver model is taken into account so as to form a closed-loop simulation enviroment. In general, the parameters of the driver model reflects not only the intrinsic driving characteristics of the driver, but also the vehicle's handling stability.

1) THE PREVIEW OPTIMAL CURVATURE DRIVER MODEL

Suppose that the vehicle is running on a predetermined road, c.f., Fig.19. At time instant t, let the vehicle's lateral displacement and lateral velocity be y and $\dot{y}$, respectively. Denote $f(t)$ as the preview point at the road center trajectory at time instant t.

Suppose that the driver's longitudinal distance is d. The corresponding forward viewing time is $T \approx \frac{d}{v}$ while the vehicle's heading angle φ is small.

The closed-loop system is shown in Fig.18. While the driver completes the preview action, it is necessary to adjust the steering wheel angle δ_{sw} so that the vehicle's driving trajectory can asymptotically track the ideal road trajectory and obtain the ideal driving curvature $1/R^*$.

The lateral displacement of the vehicle is $y(t+T)$ at time instant $t+T$. By Taylor expansion, $y(t+T)$ is

$$y(t+T) = y(t) + T\dot{y}(t) + \frac{T^2}{2}\ddot{y}(t)$$

If the driver drives the vehicle with the optimal curvature $1/R^*$ by adjusting the steering wheel, the corresponding optimal lateral acceleration $\ddot{y}^*(t)$ can be obtained

$$\ddot{y}^*(t) = \frac{2}{T^2}\left[f(t+T) - y(t) - T\dot{y}(t)\right] \tag{32}$$

TABLE 2. Driver model parameters.

parameter	value
Time lage of manipulation response T_h/s	0.1
Time lag of neuronaŕs response T_d/s	0.2
Forward viewing time T/s	1
PID controller	$k_p = 0.23$ $k_i = 0.002$ $k_d = 0.035$

The road deviation is defined as

$$e(t) = f(t+T) - y(t+T) \tag{33}$$

That is,

$$e(t) = f(t+T) - y(t) - T\dot{y}(t) \tag{34}$$

The control input of the PID controller is [40]

$$\delta^*_{sw} = \frac{2}{T^2}\left[k_p e(t) + k_i \int_0^t e(t)\,dt + k_d \frac{de(t)}{dt}\right] \tag{35}$$

Let T_d be the time lag of neuron's response and T_h be the time lage of manipulation response. According to the characteristics of human behavior, the delay element $e^{-T_d s}$ is used to represent the time required for the transmission of signals in the nervous system, and the first-order inertial element $\frac{1}{1+T_h s}$ is used to represent the inertia lag when steering wheel is operated. Therefore,

$$\frac{\delta_{sw}}{\delta^*_{sw}}(s) = \frac{e^{-T_d s}}{1+T_h s} \tag{36}$$

2) STEERING INPUT OF DOUBLE LANE CHANGE

The reference path which represents the road information is shown in Fig.20. For the vehicles trajectory, CarSim can output position values. For the desired lane change trajectory, a formula fitting method is used to give the position values in simulink. The driver model parameters are shown in Table.2. The simulation results are shown in Fig.21-Fig.23, where the longitudinal velocity of the vehicle is $20m/s$.

It can be seen from Fig.20 that the trajectory of active four wheel steer-by-wire vehicle with the nonlinear triple-step controller is accordance with the desired lane change trajectory. When the vehicle completes the double lane change maneuver and returns to its original lane, there exist only a small deviation between the vehicle's trajectory and the desired lane change trajectory. The sideslip angle is small and the yaw rate and lateral acceleration are basically in

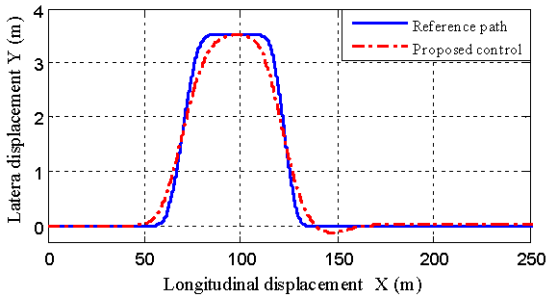

FIGURE 20. Vehicle trajectory.

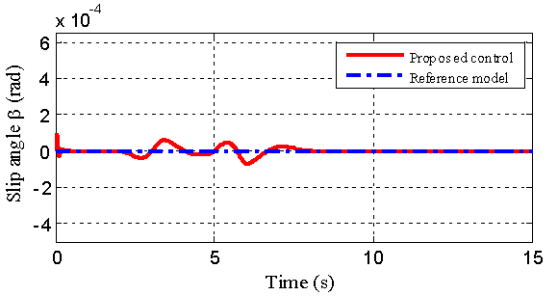

FIGURE 21. Slip angle responses.

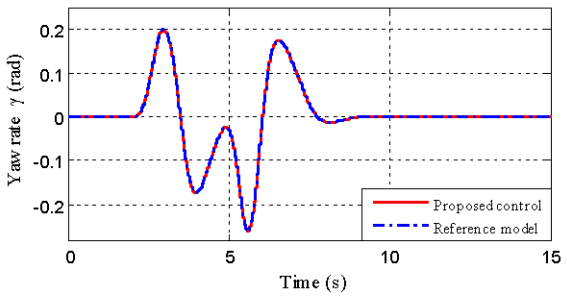

FIGURE 22. Yaw rate responses.

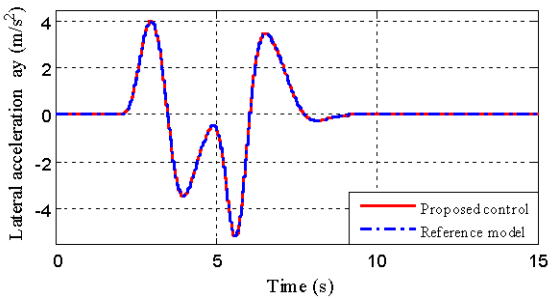

FIGURE 23. Lateral acceleration responses.

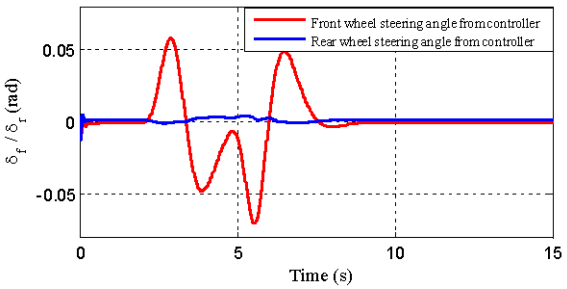

FIGURE 24. Front/Rear steering angle from controller.

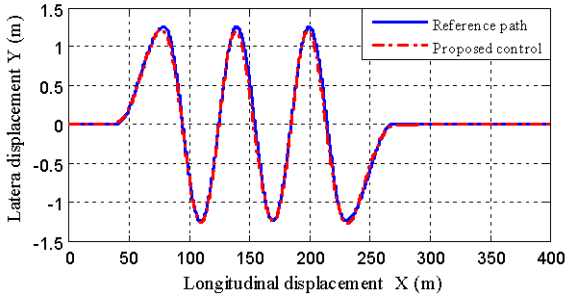

FIGURE 25. Vehicle trajectory.

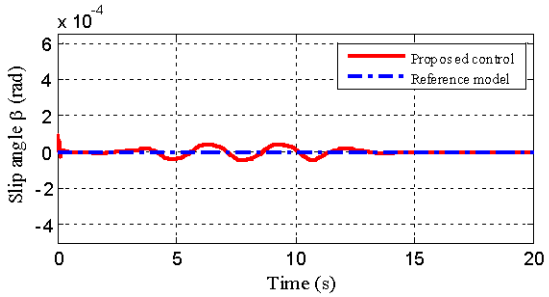

FIGURE 26. Slip angle responses.

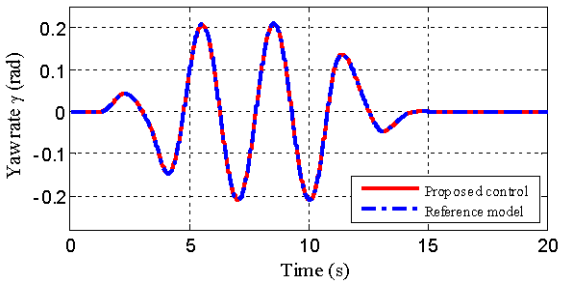

FIGURE 27. Yaw rate responses.

accordance with the ideal situation (Fig.21-Fig.23). The front and rear wheel angles always work within a reasonable range (Fig.24).

3) SERPENTINE ROAD EXPERIMENT

At human-vehicle-road closed-loop maneuverability evaluation, the serpentine road experiment reflects not only the ability of the vehicle to make a sharp turn, but also the comfort and safety of the occupant in this sharp turn. A serpentine driving experiment in CarSim is conducted at a medium-high speed of 20 m/s, and the simulation results are shown in Fig.25-Fig.29. The 4WS vehicle with the proposed controller accurately performs the tracking task on the standard serpentine path (Fig.25). As shown in Fig.26-Fig.28, the centroid sideslip angle of the vehicle is in the order of 10^{-5}, and

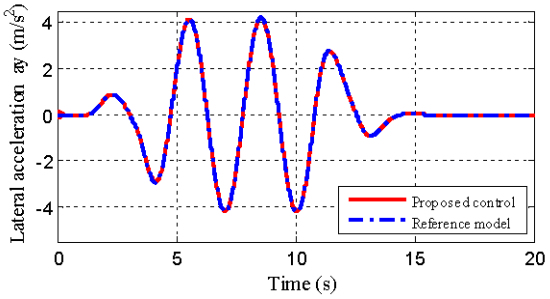

FIGURE 28. Lateral acceleration responses.

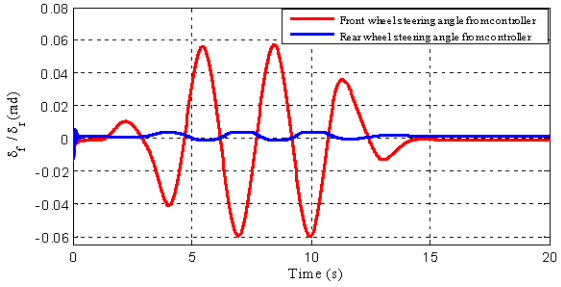

FIGURE 29. Front/Rear steering angle from controller.

the yaw rate and the lateral acceleration are in accordance with the ideal yaw rate and the lateral acceleration. The front and rear wheel angles are all within a reasonable and controllable range (Fig.29). It not only ensures a good driving feeling but also improves the safety of the vehicle during steering.

V. CONCLUSION

A triple-step controller was designed to improve the handling stability of four wheel steer-by-wire vehicles, in which nonlinear characteristics of tyres were considered. Each part of the control law contained the system output state and change parameters, and realized the self-regulation of the control law parameters. The computational complexity was reduced due to the introduction of Map. Considering the influence of the driver on the stability of the vehicle, a preview optimal curvature driver model was adopted to evaluate the vehicle handling stability. Simulation results show the effectiveness of the proposed scheme: to track accurately the dynamics of the ideal vehicles, to improve effectively the saturation margin of the tyre and to reduce dramatically the influence of uncertainties.

REFERENCES

[1] W. Sun, J. Zhang, and Z. Liu, "Two-time-scale redesign for antilock braking systems of ground vehicles," *IEEE Trans. Ind. Electron.*, vol. 66, no. 6, pp. 4577–4586, Jun. 2019.
[2] Z. Wang, J. Zhu, L. Zhang, and Y. Wang, "Automotive ABS/DYC coordinated control under complex driving conditions," *IEEE Access*, vol. 6, pp. 32769–32779, 2018.
[3] Y. Guodong, Z. Chengjie, and Z. Ning, "The torque distribution and anti-slip regulation control for two-wheel independent drive electric vehicle," in *Proc. Chin. Control Decis. Conf. (CCDC)*, May 2016, pp. 4444–4449.
[4] C. Chapuis, E. Bideaux, X. Brun, and N. Minoiu-Enache, "Comparison of feedback linearization and flatness control for anti-slip regulation (ASR) of an hybrid vehicle: From theory to experimental results," in *Proc. Eur. Control Conf. (ECC)*, Jul. 2013, pp. 446–451.
[5] H. Xiong, X. Zhu, and R. Zhang, "Energy recovery strategy numerical simulation for dual axle drive pure electric vehicle based on motor loss model and big data calculation," *Complexity*, vol. 2018, Aug. 2018, Art. no. 4071743.
[6] R.-H. Zhang, Z.-C. He, H.-W. Wang, F. You, and K.-N. Li, "Study on self-tuning tyre friction control for developing main-servo loop integrated chassis control system," *IEEE Access*, vol. 5, pp. 6649–6660, 2017.
[7] R. Zhao, W. Xie, P. K. Wong, D. Cabecinhas, and C. Silvestre, "Robust ride height control for active air suspension systems with multiple unmodeled dynamics and parametric uncertainties," *IEEE Access*, vol. 7, pp. 59185–59199, 2019.
[8] X. Sun, H. Zhang, W. Meng, R. Zhang, K. Li, and T. Peng, "Primary resonance analysis and vibration suppression for the harmonically excited nonlinear suspension system using a pair of symmetric viscoelastic buffers," *Nonlinear Dyn.*, vol. 94, no. 2, pp. 1243–1265, Oct. 2018.
[9] B. Aalizadeh, "A neurofuzzy controller for active front steering system of vehicle under road friction uncertainties," *Trans. Inst. Meas. Control*, vol. 41, no. 4, pp. 1057–1067, 2019.
[10] L. Shao, C. Jin, C. Lex, and A. Eichberger, "Robust road friction estimation during vehicle steering," *Vehicle Syst. Dyn.*, vol. 57, no. 4, pp. 493–519, 2019.
[11] N. Yuhara, "A review of four-wheel steering studies from the viewpoint of vehicle dynamics and control," *Vehicle Syst. Dyn.*, vol. 12, nos. 1–3, pp. 151–186, 2016.
[12] S. Wagner, T. Weiskircher, D. Ammon, and G. Prokop, "Pivot point-based control for active rear-wheel steering in passenger vehicles," *Vehicle Syst. Dyn.*, vol. 56, no. 8, pp. 1139–1161, 2018.
[13] M. Ataei, A. Khajepour, and S. Jeon, "A novel reconfigurable integrated vehicle stability control with omni actuation systems," *IEEE Trans. Veh. Technol.*, vol. 67, no. 4, pp. 2945–2957, Apr. 2018.
[14] G.-D. Yin, N. Chen, J.-X. Wang, and J.-S. Chen, "Robust control for 4WS vehicles considering a varying tire-road friction coefficient," *Int. J. Automot. Technol.*, vol. 11, no. 1, pp. 33–40, 2010.
[15] H. Lv and S. Liu, "Closed-loop handling stability of 4WS vehicle with yaw rate control," *J. Mech. Eng.*, vol. 59, no. 10, pp. 595–603, 2013.
[16] B. Li, S. Rakheja, and Y. Feng, "Enhancement of vehicle stability through integration of direct yaw moment and active rear steering," *Proc. Inst. Mech. Eng., D, J. Automobile Eng.*, vol. 230, no. 6, pp. 830–840, 2016.
[17] X. Wu, M. Zhang, and M. Xu, "Active tracking control for steer-by-wire system with disturbance observer," *IEEE Trans. Veh. Technol.*, vol. 68, no. 6, pp. 5483–5493, Jun. 2019.
[18] Z. Sun, J. Zheng, Z. Man, M. Fu, and R. Fu, "Nested adaptive super-twisting sliding mode control design for a vehicle steer-by-wire system," *Mech. Syst. Signal Process.*, vol. 122, pp. 658–672, May 2019.
[19] H. Zhao, B. Wang, G. Zhang, and Y. Feng, "Energy saving design and control of steering wheel system of steering by wire vehicle," *IEEE Access*, vol. 7, pp. 44307–44316, 2019.
[20] H. E. B. Russell and J. C. Gerdes, "Design of variable vehicle handling characteristics using four-wheel steer-by-wire," *IEEE Trans. Control Syst. Technol.*, vol. 24, no. 5, pp. 1529–1540, Sep. 2016.
[21] M. Canale and L. Fagiano, "Stability control of 4WS vehicles using robust IMC techniques," *Vehicle Syst. Dyn.*, vol. 46, no. 11, pp. 991–1011, 2008.
[22] L. Tan, S. Yu, Y. Guo, and H. Chen, "Sliding-Mode control of four wheel steering systems," in *Proc. IEEE Int. Conf. Mechatronics Autom.*, Aug. 2017, pp. 1250–1255.
[23] K. Shi, X. Yuan, and Q. He, "Double-layer dynamic decoupling control system for the yaw stability of four wheel steering vehicle," *Int. J. Control, Automat. Syst.*, vol. 17, no. 5, pp. 1255–1263, 2019.
[24] S. Yu, L. Tan, W. Wang, and H. Chen, "Control of active four wheel steering vehicle based on triple-step method," *J. Jilin Univ. (Eng. Technol. Ed.)*, vol. 49, no. 3, pp. 934–942, 2019.
[25] S. Yu, J. Wang, Y. Wang, and H. Chen, "Disturbance observer based control for four wheel steering vehicles with model reference," *IEEE/CAA J. Automatica Sinica*, vol. 5, no. 6, pp. 1121–1127, Nov. 2018.
[26] S. Yu, J. Wang, J.-S. Kim, H. Chen, and F. Allgöwer, "Quasi full information feedback control law of linear systems," *IFAC-PapersOnLine*, vol. 50, no. 1, pp. 904–909, 2017.
[27] F.-X. Xu, X.-H. Liu, W. Chen, C. Zhou, and B.-W. Cao, "Improving handling stability performance of four-wheel steering vehicle based on the H_2/H_∞ robust control," *Appl. Sci.*, vol. 9, no. 5, p. 857, 2019.
[28] Y. P. Liu, Y. Tang, and J. B. Bi. "Design of vehicle's controlling system used a 4WS control method based on BP neural network," *Adv. Mater. Res.*, vol. 201, pp. 276–280, Feb. 2011.

[29] S. Nan and M. Wei, "Adaptive control of active front steering and direct yaw moment for vehicle," *J. Traffic Transp. Eng.*, vol. 16, no. 3, pp. 91–99, 2016.
[30] R. Wang, G. Yin, and X. Jin, "Robust adaptive sliding mode control for nonlinear four-wheel steering autonomous Vehicles path tracking systems," in *Proc. IEEE 8th Int. Power Electron. Motion Control Conf.*, May 2016, pp. 2999–3006.
[31] G. Markkula, O. Benderius, and M. Wahde, "Comparing and validating models of driver steering behaviour in collision avoidance and vehicle stabilisation," *Vehicle Syst. Dyn.*, vol. 52, no. 12, pp. 1658–1680, 2014.
[32] S. C. Baslamisli, I. Polat, and I. E. Kose, "Gain scheduled active steering control based on a parametric bicycle model," in *Proc. IEEE Intell. Vehicles Symp.*, Jun. 2007, pp. 1168–1173.
[33] H. Chen, X. Gong, Q. Liu, and Y. Hu, "Triple-step method to design nonlinear controller for rail pressure of gasoline direct injection engines," *IET Control Theory Appl.*, vol. 8, no. 11, pp. 948–959, 2014.
[34] M. Nagai, Y. Hirano, and S. Yamanaka, "Integrated robust control of active rear wheel steering and direct yaw moment control," *Vehicle Syst. Dyn.*, vol. 29, pp. 416–421, Jan. 1998.
[35] Z. Chen, J. Zhao, Y. Hu, and H. Chen, "Design of selective catalytic reduction systems controller for diesel engine using triple-step nonlinear method," in *Proc. 11th World Congr. Intell. Control Automat.*, Jun./Jul. 2014, pp. 4724–4729.
[36] Q. Liu, H. Chen, B. Gao, and Y. Gao, "Shift control of dual clutch transmission using triple-step nonlinear method," *IFAC Proc. Volumes*, vol. 47, no. 3, pp. 5884–5889, 2014.
[37] H. Zhao, B. Gao, B. Ren, and H. Chen, "Integrated control of in-wheel motor electric vehicles using a triple-step nonlinear method," *J. Franklin Inst.*, vol. 352, no. 2, pp. 519–540, 2015.
[38] F. Wang, N. Hao, L. Song, and H. Chen, "Triple-step nonlinear control design for road vehicles after a tire blow-out on the highway," in *Proc. 12th World Congr. Intell. Control Automat.*, Jun. 2016, pp. 1414–1419.
[39] F. Yu and Y. Lin, *Automotive System Dynamics*. Beijing, China: China Machine Press, 2012.
[40] Y. Maruyama and F. Yamazaki, "Driving simulator experiment on the moving stability of an automobile under strong crosswind," *J. Wind Eng. Ind. Aerodyn.*, vol. 94, no. 4, pp. 191–205, 2006.

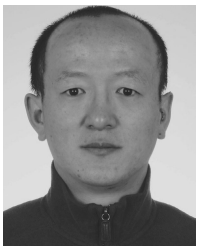

SHUYOU YU (M'12) received the B.S. and M.S. degrees in control science and engineering from Jilin University, China, in 1997 and 2005, respectively, and the Ph.D. degree in engineering cybernetics from the University of Stuttgart, Germany, in 2011. From 2010 to 2011, he was a Research and Teaching Assistant with the Institute for Systems Theory and Automatic Control, University of Stuttgart. In 2012, he joined the Department of Control Science and Engineering, Jilin University, as a Faculty Member, where he is currently a Full Professor. His main research interests include model predictive control, robust control, and its applications in mechatronic systems.

WENBO LI received the B.E. degree from the College of Communication Engineering, Jilin University, in 2019. He is currently pursuing the master's degree with the Department of Control Science and Engineering, Jilin University. His research interests include model predictive control and four-wheel steering vehicle.

WUYANG WANG received the B.E. degree from the Changchun University of Technology, China, in 2014, and the M.S. degree in control science and engineering from Jilin University, China, in 2019. During the master's degree, she mainly studied nonlinear control strategies of four-wheel steering vehicle.

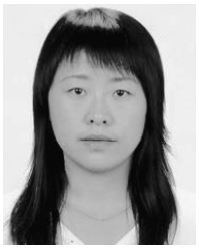

TING QU received the B.S. and M.S. degrees from Northeast Normal University, Changchun, China, in 2006 and 2008, respectively, and the Ph.D. degree in control science and engineering from Jilin University, China, in 2015, where she is currently an Associate Professor with the State Key Laboratory of Automotive Simulation and Control. Her research interests include model predictive control and driver modeling.